ISSN : 0974 - 7532 Volume 7 Issue 2

Trade Science Inc.

Research & Reviews in

BioSciences

Regular Paper

RRBS, 7(2), 2013 [76-83]

Analysis of the secondary crystalline structure of regenerated *Bombyx mori* fibroin

Edwin Kamalha*, Yuansheng Zheng, Yongchun Zeng

College of Textiles, Donghua University, 2999 North Renmin Road, 210620 Shanghai, (CHINA)

E-mail : edwinkam11@gmail.com

ABSTRACT

A protein natural biopolymer, silk possesses novel properties potential for biomedical, cosmetic and pharmaceutical applications among others. For such functions, *Bombyx mori* fibroin can be regenerated into gel, film, powder and fibers. In this study, *B.Mori* fibroin was regenerated into films and electrospun nano fibers, and their secondary structure was evaluated. Two aqueous salts (LiBr and $CaCl_2$) were fixed and used to dissolve silk fibroin, and their relative effect presented. Fourier transform infrared spectroscopy (FTIR) and Wide angle x-ray diffraction (WAXD) results showed that untreated regenerated fibroin in film and nanofibers were generally amorphous. It was thus concluded that the regeneration process has a remarkable effect on the molecular weight and crystallinity of fibroin.

KEYWORDS

Bombyx mori (B.mori);
Silk fibroin (SF);
Secondary structure;
Crystallinity;
Elecrospinning (ES);
Nano fibers.

INTRODUCTION

With a characteristic repetition of an amino acid backbone; silk I, silk II, and silk III are the three main suggested structures of fibroin. Silk I is fibroin in its natural state, while silk II-which is stronger, is the fibroin in spun silk. Silk III is a relatively recent finding and said to be basically formed in fibroin solutions at interfaces[1-3]. Three silk fibroin secondary structures reported by Jin et al.[4] include: a random structure which is not easy to align; an α-structure in absence of shear force- consisting high fibroin concentrations, and a β-structure induced under shear force or subjection to solvents, such as methanol. Orientation of the random structure to either α or β-sheet conformations can be achieved by treatment with solvents or physical shear[5]. For their secondary structure, proteins are identified commonly by the nine amide bands amide A, B, and I-VII, whereby the main vibrational bands in regard to the protein backbone are amide I and II[6,7]. In general, the FTIR bands for analyzing silk fibroin, and so for *B.mori*, have been reported to include mainly; amide I (1700-1600 cm^{-1}), amide II (1600-1500 cm^{-1}) and amide III (1300-1200 cm^{-1})[6,8-10]. Random coils and β–sheets are the main characteristic conformations of the secondary structure of *B.mori* silk fibroin[10,11]. Other studies have mentioned the α-helix as another conformation of silk fibroin, which is known to be closer to the random coils[12-15].

Regeneration processes of fibroin have been reported to impact the secondary structure of fibroin, including the crystallinity[16-19]. A study by Um and coworkers[20] on untreated regenerated fibroin revealed strong FTIR absorption bands at 1665 cm^{-1} (amide I),

1540 cm^{-1} (amide II), and 1235 cm^{-1} (amide III), assigned to random coils, and 1628 cm^{-1} (amide I), 1533 cm^{-1} (amide II) and 1265 cm^{-1} (amide III) assigned to β–sheets. Zhang et al.[21,22] studied FTIR absorption bands of water soluble silk fibroin membranes and recorded; amide I at 1654.8 cm^{-1}, amide II at 1554.1 cm^{-1}, amide III at 1242.1 cm^{-1} and amide V at 669.3 cm^{-1}, which were assigned to the random coil. With methanol treatment, shifts to β-sheet structure of these absorption bands were noted at 1635.8 cm^{-1}, 1520.0 cm^{-1}, 1238.4 cm^{-1}, and 682.9 cm^{-1} respectively. TABLE 1 is a summary of FTIR amide absorption bands, *B.mori* fibroin conformations, and their vibration nature.

TABLE 1 : Amide wave numbers and protein secondary structure[23-29].

Conformation	Amides and Wavelengths (cm^{-1})			
	A (NH stretch)	I (CO stretch)	II (NH deformation)	III (CN stretch, NH bending)
α-helix	3290-3300	1648-1660	1540-1550	1304-1313
β-sheet	3280-3300	1625-1640, 1690 weak	1520-1530	1219-1245
β-turns		1660-1685		1265-1291
Random coil	3250	1625-1660, 1640-1648	1520-1545	1257-1258
310-helix		1660-1670		1265-1291
Aggregated strands		1610-1628		

Amides- B, IV, V, VI and VII have been found in ranges of 3100 cm-1 (NH stretching), 625 cm-1-767 cm-1 (OCN bending), 640 cm-1-800 cm-1 (out-of-plane NH bending), 537 cm-1-606 cm-1 (out-of-plane C=O bending), and 200 cm-1 (skeletal torsion), respectively[30-32].

Based on the amount of observed β-sheet absorptions and the intensity of such peaks, the FTIR crystallinity, can be to estimate the amount of fibroin crystallinity33.

X-ray diffraction crystallography gives a more quantitative analysis of crystallinity and so for the secondary structure. For example; from WAXD studies, it has been recorded that that the crystallinity of fibroin in degummed *B.mori* fibers, generally lies within 40%-50%, while regenerated fibroin is generally below 40%[19,36,37].

This study focused on regenerating fibroin, including electrospinning. FTIR and WAXD were used, to study the structure of the regenerated specimens.

EXPERIMENTAL

Materials

Bombyx mori fibers were purchased in skein form, from Zhejiang province of China. Cellulose dialysis tubing (MWCO; nominal: 14000) was supplied by Shanghai Green Bird Science and Technology Co. Ltd, China. All the other reagents were supplied by Sinorpham Chemical Co. Ltd, China, and were used in their original chemical analytical grade, as supplied.

Silk dissolution and preparation SF films

For degumming purpose, *Bombyx mori* silk fibers were boiled in 0.5% (w/w)Na_2CO_3 at 100 °C for 20 minutes, three times, while rinsing in de-ionized water after each boiling. The degummed fibers were let to dry at room temperature.

In one experiment, degummed silk fibers (DS) were dissolved in 9.5M LiBr to yield 15% (w/v), and then heated at 60°C, while stirring constantly for 6 hours. The cooled silk solution was then dialyzed against distilled water using cellulose dialysis tubing for three days, to remove the lithium salts. The dialyzed solution was filtered and subjected to evaporation (at room temperature), to yield dry silk fibroin (SFLiBr). In another experiment, a solvent system consisting of $CaCl_2$: methanol:water, in the ratio of 1:2:8 was used to dissolve the degummed silk. This was also made to 15% (w/w) and followed through dialysis and evaporation to yield dry silk fibroin films (SF$CaCl_2$).

Preparation of the spinning dope and electrospinning

Separately, SFLiBr and SF$CaCl_2$ were dissolved in 98% formic acid for 6 hours, yielding a viscous polymer solution of 30% (w/v) concentration, which was then filtered. Electrospinning was done using similar fixed parameters for both kinds of SF. A 10 ml syringe, with a stainless steel needle of 0.7 mm inner diameter was used to contain the viscous dope. A DC high-voltage was then connected to the tip of the needle and the syringe was clamped onto a pump (Cole-Parmer Instrument Co., Vernon Hills IL, USA) to point in the horizontal direction. An aluminum foil sheet was clipped onto a grounded thin metal board and placed 20cm from the tip of the needle, to act as the fiber collector. All electrospinning experiments were performed at room temperature (21 °C-25 °C) and 60%-75% humidity. The polymer flow rate and applied voltage during electrospinning were 0.3 ml/hr and 15 kV respectively.

Regular Paper

Fourier transform spectroscopy (FTIR), and wide angle x-ray diffraction (WAXD)

A Nicolet NEXUS670 FTIR spectroscope (Thermo Nicolet Co., USA) was employed to study the several bands representing specific amide groups and the secondary structure of fibroin that characterize the fibroin peptide backbone, for the generated specimens. Specimens included; degummed *B.mori* fibers, SF films and electrospun fibers. The WAXD patterns of the fibroin derivatives were performed with diffraction angles, 2θ: 5°- 60°, on a D/max-2550PC diffractometer (Rigaku Co., Japan) at 40 kV and 2000 mA using Cu/K-α1 radiation.

RESULTS AND DISCUSSION

Dissolution, dialysis and electrospinning

The silk fiber easily dissolved, and after dialysis, the yellowish to orange color faded to lighter intensity. Formic acid-dissolved fibroin was yellow to brown, and got deeper with time, due to the gelation process promoted by low pH and raising temperature. Filtration was important in getting rid of particles and any precipitates in the spinning dope. The spinning solution was used in 24 hours to avoid gelation, which would have made it hard for the spinning dope to go through the needle. Random nanofibers were electrospun from both $SFCaCl_2$ and SFLiBr, in formic acid.

FTIR spectroscopy

Structural conformational analysis was the main reason for this evaluation, and it was carried out within the 4000 cm^{-1} -500 cm^{-1} range (Figure 1a-f). Based on assumption that degumming does not alter the secondary and crystalline structure of fibroin[10,19], degummed silk was used as a control/reference throughout the relevant tests.

The major absorption bands for the silk films exhibited similar shapes and close intensities, and so were the electrospun fibers. Most peaks seem to broaden and reduce in height with further processing. Variations can be attributed to the concentration differences of fibroin in each specimen's secondary form. The relative variations are also an indication of shifts in the crystallinity and conformations (α-helix, β-sheet, random coils), which are related to the peptide backbone. Our discussion was mainly centered on amide I, II and III as basic representatives for fibroin protein.

Degummed silk fibroin (DS)

Amide I was indicated between 1698 cm^{-1} (weak β-sheet) and 1622 cm^{-1} (β-sheet, strongest) representing C=O stretching. Amide II showed absorption at 1514 cm^{-1} (β-sheet), representing CN stretching and NH bending. Amide III bands, signifying the CN stretching and NH bending were between 1258 cm^{-1} (α-helix/ random coils) and 1229 cm^{-1} (β-sheet). A strong and intense amide A band is observed at 3282 cm^{-1}(β-sheet) indicating NH bending.

LiBr derived silk fibroin film (SFLiBr)

FTIR analysis showed a strong amide I peak at 1645 cm^{-1} representing a shift from β-sheet to random coil structure, when compared to the degummed fiber, initially at 1622 cm^{-1}. Amide II bands shifted from those originally in degummed fiber fibroin, to between 1535 cm^{-1} (random coil/α-helix) and 1518 cm^{-1} (β-sheet)- a shoulder. The shifts in amide III were more pronounced from 1229 cm^{-1} in DS, to another β-sheet position at1239 cm^{-1}. The amide A band initially at 3281 cm^{-1} shifted a little in wavelength, to 3283 cm^{-1} (β-sheet) but lowered by 39% in intensity.

$CaCl_2$ derived silk fibroin film ($SFCaCl_2$)

Amide I exhibited a strong absorption band between 1652 cm^{-1} and 1647 cm^{-1} (weak), assigned to random coils/unordered structure, almost the same as in SFLiBr spectra. There was also one visible amide II absorption band at 1541 cm^{-1}, corresponding to α-helix conformation. In comparison to DS and SFLiBr, this was a strong shift to random coil. Amide II was indicated at only 1242 cm^{-1} (β-sheet). A large shift in absorption was observed in amide A, from 3282 cm^{-1} initially in DS, to 3291 cm^{-1} (α-helix), with a reduction in intensity slightly higher than was observed in SFLiBr. Intensity values of peaks were generally lower in $SFCaCl_2$ than those for SFLiBr and DS. Moreover, relative to DS, the changes in absorbed wavelengths tended more to the random coil or α-helix structure in $SFCaCl_2$ than it was in SFLiBr. This is an indication of higher reduction in the crystalline secondary structure and the concentration of fibroin in $CaCl_2$ than it was in SFLiBr.

SFLiBr electrospun silk fibroin (ESLiBr)

ESLiBr showed a characteristic amide I absorp-

Regular Paper

tion peak at 1651 cm^{-1} assigned to random coils and/or α-helix. This was a shift from 1645 cm^{-1} in its previous film form of SFLiBr. Still, there was a weak band at 1717 cm^{-1} (C=O and -COOH stretching), which could be assigned to β-sheet, and traces of α-helix conformation. Amide II spectral shifts were visible at 1539 cm^{-1} (random coils, traces of β-sheet). The main amide III absorption peak observed earlier, at 1239 cm^{-1} in SFLiBr shifted to 1241 cm^{-1}(β-sheet). Amide A was exhibited at 3293 cm^{-1} (α-helix) with a much lower intensity compared to initial values in DS and SFLiBr. For example, it was less by 67% and 29%, relative to that in DS and SFLiBr respectively, although they were at different wavelengths.

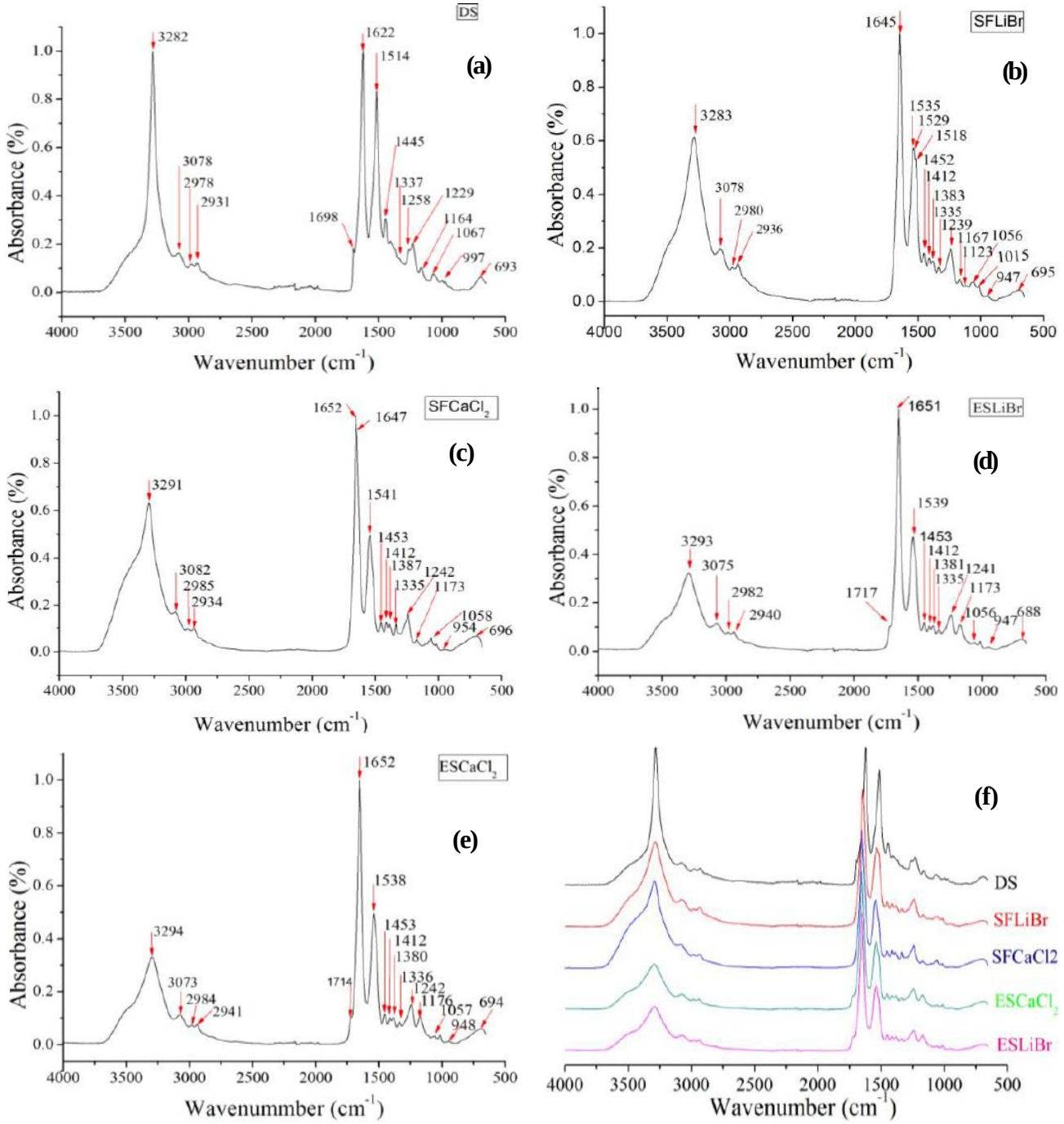

Figure 1 : Extract of individual FTIR spectra for the five specimens showing amide absorption bands: a. Degummed silk (DS) b. LiBr derived fibroin film (SFLiBr); c. CaCl2 derived fibroin film (SFCaCl2); d. Electrospun SFLiBr; e. Electrospun CaCl2. The arrows point to specific absorption bands within Amide I-V, A and B regions; f. a combined FTIR spectral analysis for the five specimens.

Regular Paper

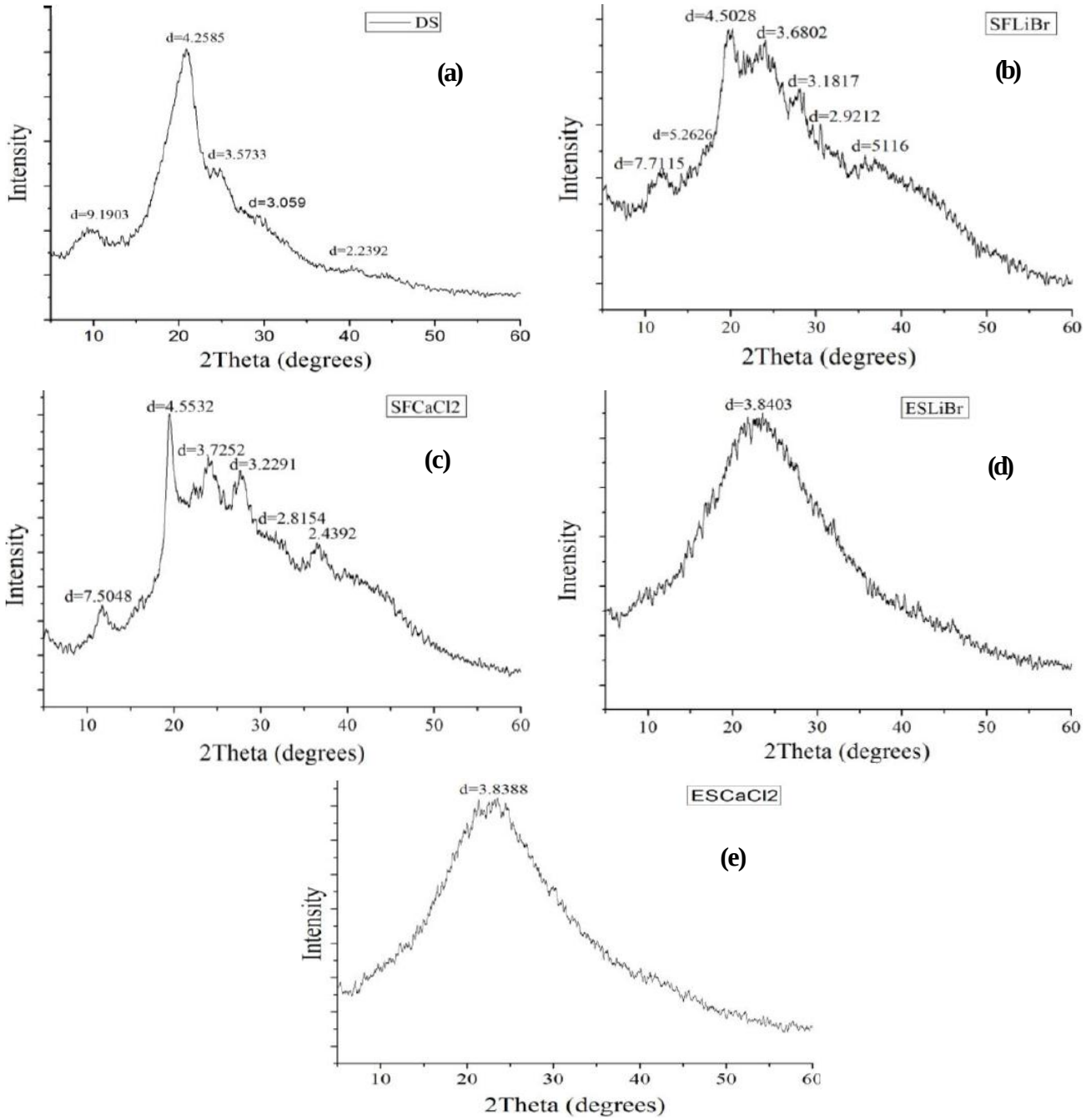

Figure 2 : Comparison of the WAXD patterns for the five specimens: a- Degummed silk (DS); b- LiBr-derived fibroin film (SFLiBr); c- CaCl2-derived fibroin film (SFCaCl2); d- Electrospun SFLiBr; e- Electrospun SFCaCl2. The Origin software-drawn curves were smoothed by the Savitzky-Golay filter.

$SFCaCl_2$ electrospun silk fibroin ($ESCaCl_2$)

The major FTIR absorption band for amide I was at 1652 cm^{-1}, almost as that in ESLiBr, both assigned to random coils and/or α-helix. The slight difference is noted in the intensity, whereby it was more pronounced in SFLiBr spectra. A characteristic β-sheet structure was recorded at 1242 cm^{-1} for amide III. An amide A absorption band is recorded at 3291 cm^{-1}(α–helix structure).

Comparing the five graphs, FTIR absorptions in amide A were between 3280 cm^{-1} and 3300 cm^{-1}, indicating a mixture of both β–sheet and α-helix structure. However, the β-sheet indications were more in DS followed by SFLiBr and then $SFCaCl_2$. They were less in electrospun fibers. Apart from the similarity in shapes of several bands, there were no clear similar peaks in terms of wavelength and intensity figures. There was progressive reduction in the intensity of prominent ab-

sorption bands, as processing went on after degumming. This may be partly attributed to loss in fibroin concentration, crystallinity and thus the molecular weight. Preliminary deduction presents fibroin in regenerated products as having more random/unordered structure than β–sheet structure, when compared to reference (degummed) fibers. From intensity of absorption bands, LiBr derivatives seem to have more β-sheet structure compared to $CaCl_2$ derived fibroin. This result could be attributed to the nature and severity of each aqueous solution.

For better conclusions, WAXD analysis was used to provide a quantitative estimate of the secondary structure crystallinity of fibroin.

Wide angle x-ray diffraction (WAXD) structural analysis

WAXD was used to predict the crystalline nature and corresponding secondary conformations for each specimen. A peak search report and analysis (TABLE 2 and Figure 2) were performed, including calculation of d-spacings (Å) and the percentage crystallinity.

TABLE 2 : Summary of the main characteristic WAXD results.

Specimen	2Theta (2θ)	d-spacing d(Å)	Conformation	Crystallinity
DS	9.616	9.1903	Silk II (β-Sheet)	46.37%
	20.956	4.2585	Silk II (β-sheet)	
	24.897	3.5733	Silk I	
SFLiBr	16.833	5.2626	Silk II(β-sheet)	19.26%
	19.700	4.5028	Silk I	
	25.166	3.5358	Silk I	
	28.021	3.1817	Silk I	
$SFCaCl_2$	15.994	5.5368	Silk I	16.26%
	19.480	4.5532	Silk I	
	21.065	4.2140	Silk II (β-sheet)	
	25.567	3.4813	Silk I	
ESLiBr	9.040	9.7747		21.64%
	22.496	3.9490	Silk I	
	23.141	3.8403		
$ESCaCl_2$	9.797	9.0204		18.28%
	23.113	3.8450	Silk I	
	23.151	3.8388		

Conformations allocated to x-ray diffractions, with reference from 10,12,13,19,30-32,34,35,38,39,42

The crystallinity values were computed using the method stated by Hermans and Weidinger[38], and Weidinger and Hermans[39]. These results show a remarkable decrease in the crystallinity of fibroin with further processing as compared to the original fiber. As earlier observed in the FTIR analysis, this is an attribute of reduced molecular weight during dissolution and dialysis of the silk.

As noted in TABLE 2, LiBr derived regenerated fibroin had higher crystallinity compared to $CaCl_2$ derived fibroin, which could be attributed to the fact that during the protein solubilization in the $CaCl_2$ ternary system, many amide bonds in the silk molecular chains undergo separation. Also, disparities in the quantity of residual salts after dialysis may cause the slight observed difference in the crystallinity of fibroin films. With increase in the concentration of fibroin, it becomes more difficult to extract more salts by dialysis. Again, lithium is particularly hasty to be dialyzed due to its high affinity for silk fibroin[40,41], hence its derivatives may show more crystallinity than $CaCl_2$ derived fibroin. Of course, there are also lapses in dissolution conditions such as temperature and time.

The slight observed increase in crystallinity of fibroin in electrospun fibers, compared to fibroin films can be explained by two factors; First, the use of formic acid during electrospinning, which induces hydrogen bonding and also re-orientation of random or helical structures to a β-sheet structure conformation. At low pH values, the fibroin undergoes gelation; an indication of increase in bonding. However, this factor was not evidently supported by the WAXD patterns of electrospun fibers, as such characteristic peaks of the β-sheet or silk II were absent. Another factor is that during electrospinning, from the time of ejection from the needle up to deposition on the collecting plate, the fibers undergo electrostatic stretch due to electric field. This causes re-alignment of molecular chains in the fibers hence contributing to some level of induced crystallinity. This factor could be solely responsible for the slight increase in crystallinity observed in the electrospun fiber fibroin compared to the films. Nevertheless, the effect of these two factors was not significant to translate into higher cystallinity compared to the DS fibroin. Most diffraction peaks in the films and electrospun fibers were a representation of silk I, which accounts for the amorphous structure of fibroin. The strongest crystalline peak, usually at 21.0o, was only observed in DS. In other specimens, this peak was either absent or shifted

Regular Paper

slightly. In general, the diffraction patterns of electrospun fibers were similar, except for the observed difference in the magnitudes of crystallinity. This fact is also true for the fibroin films.

CONCLUSION

Silk fibroin was successfully regenerated using concentrated aqueous lithium bromide solution and a neutral $CaCl_2$:Water:Ethanol system. Collaboration of FTIR and X-ray results revealed that there is an appreciable amount of fibroin that is contained in regenerated silk. This fibroin, without treatment, is mainly silk I, characterized by mainly random coils and α-helix structure. Also, the electrospinning process does induce some β-sheet crystallinity to nanofibers, through intra hydrogen bonding due to acid effect, and re-alignment caused by electric field stretching. Our findings suggest that the type of solvent used to dissolve silk has insignificant effect on the structure of nanofibers, and regenerated fibroin. Results also imply that fibroin undergoes degradation (loss of molecular weight) and loss of secondary structure crystallinity during regeneration. Hence, an aqueous environment also facilitates the transition to a random structure. Lastly, it was found that untreated regenerated fibroin is largely amorphous. Our results are partially consistent with findings by Zarkoob et al.[17] and Wang et al.[18].

AREAS FOR FURTHER STUDY

We observed that the dissolution properties largely influence the molecular weight of regenerated fibroin. Our ongoing study is exploring the effect of factors including dissolution temperature and dissolution time on the secondary structure of silk fibroin. We are also studying treatments to improve crystallinity of regenerated fibroin.

ACKNOWLEDGMENT

This research was supported by the National Natural Science Foundation of China (grant number: 10972052); Foundation for the Author of National Excellent Doctoral Dissertation of the People's Republic of China (grant number: 2007B54); New Century Excellent Talents Plan of Chinese Ministry (grant number: NCET-09-0285); Shanghai Dawning Program (grant number: 10SG33).

REFERENCES

[1] W.H.Parka, L.Jeonga, D.Yoob, S.Hudson; Polymer, **45**, 7151 **(2004)**.
[2] http://en.wikipedia.org/wiki/Fibroin (retrieved on April 25, 2012).
[3] R.Valluzzi, S.P.Gido, W.Muller, D.L.Kaplan; Int.J.Biol.Macromol., **24**, 237 **(1999)**.
[4] H.J.Jin, D.L.Kaplan; Nature, **424**, 1057 **(2003)**.
[5] S.J.He, R.Valluzzi, S.P.Gido; Int.J.Biol.Macromol., **24**, 187 **(1999)**.
[6] B.Stuart; Infrared spectroscopy, fundamentals and applications, 1st Edition, Wiley, New York, **(2004)**.
[7] L.H.Kidder, A.S.Haka, E.N.Lewis; In instrumentation for FT-IR imaging, handbook of vibrational spectroscopy, J.M.Chalmers, P.R.Griffiths (Eds); Wiley, Chichester, **2**, 1386-1404 **(2002)**.
[8] S.Krimm, J.Bandekar; Adv.Protein Chem., **38**, 18 **(1986)**.
[9] W.K.Surewicz, H.H.Mantsch; Biochim Biophys Acta, **952**, 115 **(1988)**.
[10] T.Asakura, A.Kuzuhara, R.Tabeta, H.Saito; Macromolecules, **18**, 1841 **(1985)**.
[11] X.Chen, Z.Shao, N.S.Marinkovic, L.M.Miller, P.Zhou, M.R.Chance; Biophys Chem., **89**, 25 **(2001)**.
[12] J.He, Y.Qin, S.Cui, Y.Gao, S.Wang; J.Mater.Sci., **46**, 2938 **(2011)**.
[13] M.M.R.Khan, Y.Gotoh, H.Morikawa, M.Miura; Fiber Polym., **7(4)**, 333 **(2006)**.
[14] W.Tao, M.Li, C.Zhao; Int.J.Biol.Macromol, **40(5)**, 472 **(2007)**.
[15] H.Kweon, Y.H.Park; J.Appl.Polym.Sci., **82**, 750 **(2001)**.
[16] H.J.Jin D.L.Kaplan; Nature, **424**, 1057 **(2003)**.
[17] S.Zarkoob, D.H.Reneker, R.K.Eby, S.D.Hudson, D.Ertley, W.W.Adams; Polym.Prepr., **39(2)**, 244 **(1998)**.
[18] M.Wang, H.J.Jin, D.L.Kaplan, G.C.Rutledge; Macromolecules, **37(18)**, 6856 **(2004)**.
[19] J.Ayutsede, M.Gandhi, S.Sukigara, M.Micklus, H.E.Chen, F.Ko; Polymer., **46**, 1625 **(2005)**.
[20] I.C.Um, H.Y.Kweon, K.G.Lee, Y.H.Park; Int.J.Biol.Macromol, **33**, 203 **(2003)**.
[21] Y.Q.Zhang, W.D.Shen, R.L.Xiang, L.J.Zhuge, W.J.Gao, W.B.Wang; J.Nanopart Res., **9**, 885 **(2007)**.

[22] Y.Q.Zhang, J.Zhu, R.A.Gu; Appl.Biochem. Biotechnol., **75**, 215 **(1998)**.
[23] C.L.Wilder, A.D.Friedrich, R.O.Pons, G.O.Daumy, M.L.Francoeur; Biochemistry, **31**, 27 **(1992)**.
[24] M.Jackson, H.H.Mantsch; Crit.Rev.Biochem. Mol.Biol., **30(2)**, 95 **(1995)**.
[25] A.Barth; Prog.Biophys.Mol.Biol., **74**, 141 **(2000)**.
[26] D.M.Byler, H.Susi; Biopolymers., **25(3)**, 469 **(1986)**.
[27] J.Kong, S.Yu; Acta Biochimica.et Biophysica. Sinica., **39(8)**, 549 **(2007)**.
[28] L.K.Tamm S.A.Tatulian; Q.Rev.Biophys., **30(4)**, 365 **(1997)**.
[29] C.R.Cantor P.R.Schimmel; Biophysical chemistry, part II: Techniques for the study of biological structure and function, WH Freeman & Co, San Francisco, **(1980)**.
[30] A.Elliott E.J.Ambrose; Nature, **165**, 921 **(1950)**.
[31] S.Krimm J.Bandekar; Adv.Protein Chem., **38**, 181 **(1986)**.
[32] J.Banker; Biochim.Biophys.Acta, **1120**, 123 **(1992)**.
[33] G.Susanne, K.Hartmut, R.Christian, W.Paul, L.Sophia in; Scientific analysis of ancient and historic textiles, First annual conference of the AHRC research centre for textile conservation and textile studies, J.Rob, W.Paul (Ed); London, UK, Archetype, 38-43 **(2005)**.
[34] N.Reddy, Y.Yang; J.Mater.Sci., **45**, 6617 **(2010)**.
[35] E.Iizuka; Biorheology, **3**, 1-8 **(1965)**.
[36] Y.Q.Zhang, W.D.Shen, J.P.Mao; China Patent, CN1443840, **(2003)**.
[37] Y.Q.Zhang, J.Zhu, R.A.Gu; Appl.Biochem. Biotechnol., **75**, 215 **(1998)**.
[38] P.H.Hermans, A.Weidinger; J.Appl.Phys., **19(5)**, 491 **(1948)**.
[39] A.Weidinger, P.H.Hermans; Die Makromoleculare Chemie., **50**, 98 **(1961)**.
[40] S.W.Ha, Y.H.Park, S.M.Hudson; Biomacromolecules, **4**, 488 **(2003)**.
[41] Y.Q.Zhang, W.D.Shen, R.L.Xiang, L.J.Zhuge, W.J.Gao, W.B.Wang; J.Nanopart Res., **9**, 885 **(2007)**.
[42] J.Nam, Y.H.Park; J.Appl.Polym.Sci., **81**, 3008 **(2001)**.